Activation of C_2H_6 and C_3H_8 by Gas-Phase Mo^+: Potential Energy Surfaces and Reaction Mechanisms

P. B. Armentrout*

Department of Chemistry, University of Utah, Salt Lake City, Utah 84112

Received June 12, 2007

A theoretical investigation of the reaction mechanisms for C−H and C−C bond activation processes in the reaction of Mo^+ (^6S) with ethane and propane is carried out. Results obtained at the B3LYP/HW/6-311++G(3df,3p) level of theory are compared with guided ion beam mass spectrometry studies provided in the preceding paper. A complete exploration of the potential energy surfaces is conducted for ethane, whereas some limitations are imposed on calculations for the more complicated propane system. In all cases, intermediates and transition states along the reaction paths of interest are characterized. It is found that both the C−H and C−C bond activation processes are limited by the initial activation step, with a transition state having an energy in reasonable agreement with experimental observations. The rate-limiting TS is located on the quartet surface for C−H activation and on the sextet surface for C−C activation. This difference can be traced to the directionality of the sp^3-hybridized orbital on methyl compared to the spherical orbital on the H atom, which raises the relative energy on the quartet surface, where the metal ion binds covalently to both fragments, but less so on the sextet surface, where one of the fragments is not covalently bound to Mo^+. In the propane system, the calculations show that methane elimination can plausibly occur either by initial C−C or C−H bond activation, although the former pathway seems more likely.

Introduction

In the preceding paper (Paper I),[1] the reactivity of Mo^+ over a wide range of kinetic energies is quantitatively characterized using guided ion beam mass spectrometry. In addition to outlining the experimental observations, this paper extracts systematic thermodynamic information for the various product ions observed and compares these results to an extensive set of theoretical calculations. However, in order to thoroughly address the question of Schilling and Beauchamp, "What is wrong with gas-phase chromium? A comparison of the unreactive chromium (1+) cation with the alkane-activating molybdenum cation",[2] the mechanism of these reactions also needs to be explored. Although the experimental results provide a great deal of mechanistic insight, they cannot provide details of the mechanisms because multiple pathways are available. Hence, the present work uses theoretical methods to explore the potential energy surfaces for interaction of Mo^+ with ethane and propane in order to help resolve mechanistic details for these reactions. This work builds on a similar theoretical exploration of the potential energy surfaces for reaction of Mo^+ with methane.[3]

Determining reaction mechanisms is one of the more challenging problems in the study of alkane activation by transition metal ions. Detailed experimental[4−8] and theoretical[9−13] studies of first-row transition metal cations (mostly Fe^+, Co^+, and Ni^+) have been carried out to elucidate mechanisms, whereas many fewer studies that emphasize mechanisms for second-row transition metal cations have been performed.[3,9,14−16] Nevertheless, it is clear that the mechanisms do vary, both from early to late and from first-row to second-row transition metal cations, as reviewed elsewhere.[17] Previous work on Cr^+, the first-row congener of Mo^+, has presumed that the mechanisms for the low-energy processes observed involve oxidative addition processes followed by reductive elimination of H_2 and small alkanes.[18−20] The present study utilizes the enhanced availability of theory to explore such assumptions in much more detail for the Mo^+ system.

It should be noted that crossings between surfaces of different spin are significant in this system (and indeed in many transition metal systems), and therefore it is possible that the reactions discussed are limited by these curve crossings rather than by transition states. Explicit calculation of the location of these

* Corresponding author: Fax (801) 581-8433; e-mail: armentrout@chem.utah.edu.

(1) Armentrout, P. B. *Organometallics* **2007**, *26*, 5473.
(2) Schilling, J. B.; Beauchamp, J. L. *Organometallics* **1988**, *7*, 194.
(3) Armentrout, P. B. *J. Phys. Chem. A* **2006**, *110*, 8327−8338.
(4) van Koppen, P. A. M.; Brodbelt-Lustig, J.; Bowers, M. T.; Dearden, D. V.; Beauchamp, J. L.; Fisher, E. R.; Armentrout, P. B. *J. Am. Chem. Soc*. **1990**, *112*, 5663; **1991**, *113*, 2359.
(5) van Koppen, P. A. M; Bowers, M. T.; Fisher, E. R.; Armentrout, P. B. *J. Am. Chem. Soc*. **1994**, *116*, 3780.
(6) van Koppen, P. A. M.; Bowers, M. T.; Haynes, C. L.; Armentrout, P. B. *J. Am. Chem. Soc*. **1998**, *120*, 5704.
(7) Haynes, C. L.; Fisher, E. R.; Armentrout, P. B. *J. Phys. Chem*. **1996**, *100*, 18300.
(8) Noll, R. J.; Yi, S. S.; Weisshaar, J. C. *J. Phys. Chem*. **1998**, *102*, 386.
(9) Perry, J. K. Ph.D. Thesis, Caltech, 1994.
(10) Holthausen, M. C.; Fiedler, A.; Schwarz, H.; Koch, W. *J. Phys. Chem*. **1996**, *100*, 6236.
(11) Holthausen, M. C.; Koch, W. *Helv. Chim. Acta* **1996**, *79*, 1939.
(12) Holthausen, M. C.; Koch, W. *J. Am. Chem. Soc*. **1996**, *118*, 9932.
(13) Yi, S. S.; Blomberg, M. R. A.; Siegbahn, P. E. M.; Weisshaar, J. C. *J. Phys. Chem*. **1998**, *102*, 395.
(14) Blomberg, M. R. A.; Siegbahn, P. E. M.; Svensson, M. *J. Phys. Chem*. **1994**, *98*, 2062.
(15) Chen, Y.-M.; Armentrout, P. B. *J. Phys. Chem*. **1995**, *99*, 10775.
(16) Chen, Y.-M.; Armentrout, P. B. *J. Am. Chem. Soc*. **1995**, *117*, 9291.
(17) Armentrout, P. B. In *Organometallic Bonding and Reactivity*; Brown, J. M., Hofmann, P., Eds.; Topics in Organometallic Chemistry, Vol. 4; Springer-Verlag: Berlin, 1999; pp 1−45.
(18) Georgiadis, R.; Armentrout, P. B. *Int. J. Mass Spectrom. Ion Processes* **1989**, *89*, 227−247.
(19) Fisher, E. R.; Armentrout, P. B. J. *Am. Chem. Soc*. **1992**, *114*, 2039−2049.
(20) Fisher, E. R.; Armentrout, P. B. *J. Am. Chem. Soc*. **1992**, *114*, 2049−2055.

10.1021/om700578q CCC: $37.00 © 2007 American Chemical Society
Publication on Web 10/11/2007

curve crossings is beyond the scope of the present work. However, most of the mechanistic conclusions arrived at below are achieved by favorable comparison of the experimental thresholds with calculated transition state energies. Thus, although curve crossings can influence the energy dependence of the observed cross sections (as explicitly demonstrated for the reaction of Mo^+ with methane),[3] in many cases, the thresholds accurately reflect the rate-limiting transition states.

Theoretical Section

All quantum chemistry calculations here are computed with the B3LYP hybrid density functional method[21−23] and are performed with the Gaussian 03 suite of programs.[24] In all cases, the thermochemistry reported here is corrected for zero-point energy (ZPE) effects (with frequencies scaled by 0.989).[25] Because the transition states of interest here often involve bridging hydrogens, the rather large 6-311++G(3df,3p) basis set is used for carbon and hydrogen. As noted in Paper I,[1] this basis set gives good results for the thermochemistry of ethane and dihydrogen. The basis set on molybdenum was the Hay−Wadt (n+1) ECP VDZ (designated as HW),[26] equivalent to the Los Alamos ECP (LANL2DZ) basis set, in which 28 core electrons are described by a relativistic effective core potential (ECP).[27] The combination of these two basis sets is designated as HW/6-311++G(3df,3p).

In our recent study of the reactions of Mo^+ with methane,[3] the thermochemistry of MoH^+ and $MoCH_x^+$ ($x = 0-3$) was carefully examined at several levels of theory: B3LYP, Becke half and half LYP (BHLYP),[28,29] MP2(full),[30] and QCISD(T)[31] approaches using the HW, HW*, and Stuttgart−Dresden (SD) ECPs and basis sets.[32] The best agreement between experiment and theory was achieved with the B3LYP and QCISD(T) approaches, with the latter giving slightly better agreement. In the preceding paper, $MoC_2H_x^+$ (x = 1−5) were studied using these two approaches with the HW and HW* basis set on Mo. For all of the molybdenum species examined to date, the HW* basis set for molybdenum gave comparable results that were slightly better than those for the HW basis (but only by about 0.03 eV on average). For the more complicated species examined in this work, we limited our calculations to the B3LYP/HW/6-311++G(3df,3p) level. As discussed in Paper I, this level of theory provides reasonable agreement with the experimental bond dissociation energies measured there (average differences of about 0.3 eV).[1] Further, it predicts the excitation energy of the $^4G(4d^5)$ state to be 1.924 eV, in excellent agreement with the experimental value of 1.906 eV,[33] although the $^6D(5s^14d^4)$ excitation energy of 1.587 eV is overestimated at 2.255 eV.[3]

For many of the species examined here, calculations of excited states were obtained by explicitly moving electrons into other orbitals to create states of alternate configuration and/or symmetry. Optimizations of the geometry were then carried out in the usual way. Identification of stationary points on the potential energy surfaces was verified by frequency calculations in all cases. Transition states were generally located using relaxed potential energy surface scans that also verify that these transition states connect the intermediates of interest.

Reaction Mechanisms

Qualitative Considerations. The activation of alkanes by transition metal cations is generally explained using an oxidative addition mechanism in which M^+ inserts into a C−H or C−C bond to form $R-M^+-H$ or $R'-M^+-CH_3$ intermediates.[17,34] Products can be formed by reductive elimination of small molecules such as H_2 and CH_4 at low energies and by metal−hydrogen or metal−carbon bond cleavage at high energies. The elimination processes can occur either by multicenter transition states or by rearrangement of the intermediate through β-H or β-CH_3 transfers to form $(H)_2M^+(C_xH_{2x})$ or $(H)(CH_3)M^+(C_{x-1}H_{2x-2})$ species, which then reductively eliminate H_2 or CH_4, respectively. This general mechanism has also been invoked to interpret experimental observations for the reactions of the first-row transition metal congener, Cr^+, with alkanes.[18−20] Among the key issues in determining the detailed mechanism is the spin states of the reactant, intermediates, and products and the stabilities of two types of possible intermediates: (a) $R-Mo^+-H$ and $R'-Mo^+-CH_3$, and (b) $(H)_2Mo^+(C_xH_{2x})$ and $(H)(CH_3)Mo^+(C_{x-1}H_{2x-2})$.

The reactants in the experiments have a sextet spin state, $Mo^+(^6S) + C_xH_{2x+2}$ (^1A). Previous calculations (and confirmed in Paper I) indicate that the ground state of MoH^+ is $^5\Sigma^+$,[1,3,35−37] MoH is $^6\Sigma^+$,[38−40] $MoCH_3^+$ is $^5A_1$,[3,39] $MoCH_2^+$ is $^4B_1$,[3,41]

(21) Becke, A. D. *J. Chem. Phys.* **1993**, *98*, 5648.
(22) Lee, C.; Yang, W.; Parr, R. G. *Phys. Rev. B* **1988**, *37*, 785.
(23) Stephens, P. J.; Devlin, F. J.; Chabalowski, C. F.; Frisch, M. J. *J. Phys. Chem.* **1994**, *98*, 11623.
(24) Frisch, M. J.; Trucks, G. W.; Schlegel, H. B.; Scuseria, G. E.; Robb, M. A.; Cheeseman, J. R.; Montgomery, J. A., Jr.; Vreven, T.; Kudin, K. N.; Burant, J. C.; Millam, J. M.; Iyengar, S. S.; Tomasi, J.; Barone, V.; Mennucci, B.; Cossi, M.; Scalmani, G.; Rega, N.; Petersson, G. A.; Nakatsuji, H.; Hada, M.; Ehara, M.; Toyota, K.; Fukuda, R.; Hasegawa, J.; Ishida, M.; Nakajima, T.; Honda, Y.; Kitao, O.; Nakai, H.; Klene, M.; Li, X.; Knox, J. E.; Hratchian, H. P.; Cross, J. B.; Bakken, V.; Adamo, C.; Jaramillo, J.; Gomperts, R.; Stratmann, R. E.; Yazyev, O.; Austin, A. J.; Cammi, R.; Pomelli, C.; Ochterski, J. W.; Ayala, P. Y.; Morokuma, K.; Voth, G. A.; Salvador, P.; Dannenberg, J. J.; Zakrzewski, V. G.; Dapprich, S.; Daniels, A. D.; Strain, M. C.; Farkas, O.; Malick, D. K.; Rabuck, A. D.; Raghavachari, K.; Foresman, J. B.; Ortiz, J. V.; Cui, Q.; Baboul, A. G.; Clifford, S.; Cioslowski, J.; Stefanov, B. B.; Liu, G.; Liashenko, A.; Piskorz, P.; Komaromi, I.; Martin, R. L.; Fox, D. J.; Keith, T.; Al-Laham, M. A.; Peng, C. Y.; Nanayakkara, A.; Challacombe, M.; Gill, P. M. W.; Johnson, B.; Chen, W.; Wong, M. W.; Gonzalez, C.; Pople, J. A. *Gaussian 03*, Revision B.02; Gaussian, Inc.: Wallingford, CT, 2004.
(25) Foresman, J. B.; Frisch, Æ. *Exploring Chemistry with Electronic Structure Methods*, 2nd ed.; Gaussian: Pittsburgh, 1996.
(26) Hay, P. J.; Wadt, W. R. *J. Chem. Phys.* **1995**, *82*, 299.
(27) The basis sets used for Mo were obtained from the Extensible Computational Chemistry Environment Basis Set Database, Version 10/29/02, as developed and distributed by the Molecular Science Computing Facility, Environmental and Molecular Sciences Laboratory, which is part of the Pacific Northwest Laboratory, P.O. Box 999, Richland, WA 99352, and funded by the U.S. Department of Energy. The Pacific Northwest Laboratory is a multiprogram laboratory operated by Battelle Memorial Institute for the U.S. Department of Energy under contract DE-AC06-76RLO 1830.
(28) Holthausen, M. C.; Heinemann, C.; Cornehl, H. H.; Koch, W.; Schwarz, H. *J. Chem. Phys.* **1995**, *102*, 4931.
(29) Holthausen, M. C.; Mohr, M.; Koch, W. *Chem. Phys. Lett.* **1995**, *240*, 245.
(30) Møller, C.; Plesset, M. S. *Phys. Rev.* **1934**, *46*, 618.
(31) Pople, J. A.; Head-Gordon, M.; Raghavachari, K. *J. Chem. Phys.* **1987**, *87*, 5968.
(32) Andrae, D.; Haeussermann, U.; Dolg, M.; Stoll, H.; Preuss H. *Theor. Chim. Acta* **1990**, *77*, 123.
(33) Moore, C. E. *Atomic Energy Levels*; NSRDS-NBS 35, 1971; Vol. III, p 1.
(34) For, reviews, see: Armentrout, P. B. In *Selective Hydrocarbon Activation: Principles and Progress*; Davies, J. A., Watson, P. L., Greenberg, A., Liebman, J. F., Eds.: VCH: New York, 1990; p 467. Armentrout, P. B. In *Gas Phase Inorganic Chemistry*; Russell, D. H., Ed.; Plenum: New York, 1989; p 1. Armentrout, P. B.; Beauchamp, J. L. *Acc. Chem. Res.* **1989**, *22*, 315. Armentrout, P. B. *Science* **1991**, *251*, 175. Armentrout, P. B. *Annu. Rev. Phys. Chem.* **1990**, *41*, 313.
(35) Schilling, J. B.; Goddard, W. A., III; Beauchamp, J. L. *J. Am. Chem. Soc.* **1987**, *109*, 5565.
(36) Pettersson, L. G. M.; Bauschlicher, C. W., Jr.; Langhoff, S. R.; Partridge, H. *J. Chem. Phys.* **1987**, *87*, 481.
(37) Siegbahn, P. E. M.; Blomberg, M. R. A.; Svensson, M. *Chem. Phys. Lett.* **1994**, *223*, 35.
(38) Langhoff, S. R.; Pettersson, L. G. M.; Bauschlicher, C. W., Jr. *J. Chem. Phys.* **1987**, *86*, 268.
(39) Bauschlicher, C. W., Jr.; Langhoff, S. R.; Partridge, H.; Barnes, L. A. *J. Chem. Phys.* **1989**, *91*, 2399.
(40) Balasubramanian, K. *J. Chem. Phys.* **1990**, *93*, 8061.

$Mo(H_2)^+$ is $^6A_1$ and $Mo(H)_2^+$ is $^4B_2$,[1,42] and $Mo(H)(CH_3)^+$ is $^4A'$.[3,14] For $Mo^+(C_2H_4)$, we calculate a $^6A_1$ ground state, whereas $Mo(C_2H_2)^+$ is calculated to have a $^4A_2$ ground state with a low-lying $^6A_1$ excited state.[1] The only other primary product is $MoC_2H_5^+$, which has a $^5A'$ ground state,[1] similar to that for $MoCH_3^+$. For the remaining secondary products, we calculate a $^3\Sigma^-$ ground state for $MoCH^+$,[3] $^5\Sigma^+$ for MoC_2H^+, $^5A''$ for $MoC_2H_3^+$, and ^3A for $HMo^+(C_2H_2)$.[1] Thus, formation of the $MoH + C_xH_{2x+1}^+$, $MoH^+ + C_xH_{2x+1}$, $MoCH_3^+ + C_{x-1}H_{2x-1}$, and $MoC_2H_5^+ + CH_3$ products is spin-allowed, as is dehydrogenation to form Mo^+(alkene) products. Notably, formation of $MoCH_2^+ + C_{x-1}H_{2x}$ and the $Mo^+(C_xH_{2x-2}) + 2H_2$ reactions are spin-forbidden, as well as several of the higher order subsequent dehydrogenation processes forming $MoCH^+$ and $HMo^+(C_2H_2)$. We can also determine that the $R-Mo^+-H$ and $R'-Mo^+-CH_3$ intermediates should have quartet spin ground states, in direct analogy with $Mo(H)_2^+$ and $Mo(H)(CH_3)^+$, a conclusion confirmed by additional calculations of $HMoC_xH_{2x+1}^+$ and $Mo(CH_3)(C_{x-1}H_{2x-1})^+$ discussed below. Likewise, the possible $(H)_2Mo^+(C_xH_{2x})$ and $(H)(CH_3)Mo^+(C_{x-1}H_{2x-2})$ intermediates are expected to have quartet ground states, as confirmed below for $(H)_2Mo^+(C_2H_4)$ and $(H)(CH_3)Mo^+(C_2H_4)$. In both alkane systems, this indicates that there is a change in spin from sextet to quartet as the reactants interact strongly with the alkane to form the $R-Mo^+-H$ and $R'-Mo^+-CH_3$ intermediates. Most subsequent rearrangements and the formation of most products can then evolve along quartet surfaces, with the Mo^+(alkene) products being a notable exception, as these must cross back to a sextet surface in order to form ground state products.

As noted in Paper I,[1] there is strong competition observed between the formation of the thermodynamically favored products, e.g., $MoC_2H_4^+ + H_2$ and $MoC_3H_6^+ + H_2$, and the $MoH^+ + R$ products. A key observation is that the decline in the cross sections of the former products is compensated by the increase in the MoH^+ cross section. Although contributions of direct abstraction processes to the formation of MoH^+ cannot be excluded, such a mechanism is unlikely to compete so efficiently with the dehydrogenation channels. However, if these processes share a common intermediate and $MoH^+ + R$ formation is kinetically favored, then this process will rapidly deplete the intermediate before the more complicated dehydrogenation reactions can occur. The $H-Mo^+-R$ intermediate is an obvious choice, as MoH^+ formation can occur by simple bond cleavage at elevated kinetic energies, whereas H_2 elimination must occur by a more restricted transition state. Thus, the existence of this intermediate is experimentally demonstrated for Mo^+ reacting with any alkane.[1,3] Likewise, the existence of CH_3-Mo^+-R' intermediates seems certain, as these lead to the primary $MoCH_3^+$ and $MoC_2H_5^+$ products observed in the ethane and propane systems. The mechanisms responsible for the dehydrogenation and alkane elimination reactions observed at low energy are more difficult to determine and are discussed in the following sections.

Dehydrogenation of Ethane: $Mo^+(C_2H_4) + H_2$ Formation. Dehydrogenation of the alkanes can proceed by initial C−H bond activation to form $H-Mo^+-C_xH_{2x+1}$. This intermediate can then rearrange through a multicenter transition state in which a β-H interacts directly with the H on the metal to yield a (H_2)-$Mo^+(C_xH_{2x})$ complex. Alternatively, the β-H first transfers to the metal to form $(H)_2Mo^+(C_xH_{2x})$, which then reductively eliminates H_2, again forming $(H_2)Mo^+(C_xH_{2x})$. This latter product generally loses the H_2 ligand, as it is bound much less strongly than the alkene (BDEs of 0.14 vs >0.8 eV).[1] Despite this large difference in binding energies, a small amount of $Mo(H_2)^+$ is generated by competitive loss of the alkene in the ethane system. These qualitative concepts can be further explored by using theory, B3LYP/HW/6-311++G(3df,3p), to examine the potential energy surface for dehydrogenation of ethane. The results are shown in Figure 1 and include all pertinent intermediates and transition states along the sextet and quartet surfaces. Geometries of the intermediates are shown in Figure 2 (and more completely tabulated in the Supporting Information, Table S1), and their energies are given in Table 1.

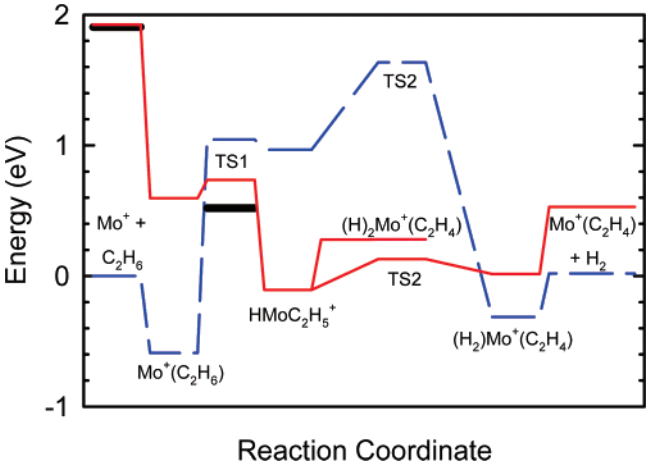

Figure 1. $[Mo,2C,6H]^+$ potential energy surfaces for CH bond activation derived from theoretical results. Sextet spin surfaces are indicated by the blue dashed line and quartet spin surfaces by the red full line. The energies of all species relative to the Mo^+ (^6S) + C_2H_6 ground state asymptote are based on ab initio calculations (B3LYP/HW/6-311++G(3df,3p), see Table 1). Heavy horizontal lines indicate experimentally measured values.

As expected, the initial interaction of Mo^+ with ethane is attractive because of the ion-induced dipole potential. The well on the sextet surface (0.59 eV) is shallower than on the quartet surface (1.33 eV), which reflects the ability of the $^4G(4d^5)$ configuration to efficiently accept electron density because of the empty 5s and 4d orbitals, whereas the $^6S(4d^5)$ configuration has only the empty 5s orbital to accept electrons. Both the $^6A'$ and $^4A'$ states of $Mo^+(C_2H_6)$ are similar to comparable spin states of $Mo^+(CH_4)$, which have A_1 ground states with C_{2v} symmetry. Substitution of one of the hydrogen atoms pointing away from the molybdenum by a methyl group yields the structures shown in Figure 2, both of which have C_s symmetry. Excited states of the $Mo^+(C_2H_6)$ complex were also located and include $^4A''$, $^2A'$, $^6A''$, and $^2A''$, Tables 1 and S1. Our $Mo^+-C_2H_6$ bond energy of 0.59 eV is somewhat greater than that previously calculated by Rosi et al. (0.39 eV).[41]

From the $Mo^+(C_2H_6)$ intermediates, activation of a C−H bond occurs through transition state TS1. This forms the $HMoC_2H_5^+$ intermediates, which now have a quartet ground state lying 1.07 eV below the sextet state and 0.11 eV below ground state reactants. The quartet state is more stable than the sextet state because the high spin of the sextet state does not allow formation of two covalent bonds. Hence in the sextet state, the MoH bond length of 1.68 Å is only slightly longer than that in MoH^+ ($^5\Sigma^+$), 1.67 Å, whereas the MoC bond length of 2.49 Å is much longer than that for $MoC_2H_5^+$ ($^5A'$), 2.11 Å. In contrast, the quartet state of $HMoC_2H_5^+$ has bond lengths of 1.67 and 2.09 Å, respectively, quite comparable to those of MoH^+ and $MoC_2H_5^+$,

(41) Rosi, M.; Bauschlicher, C. W., Jr.; Langhoff, S. R.; Partridge, H. *J. Phys. Chem.* **1990**, *94*, 8656.
(42) Das, K. K.; Balasubramanian, K. *J. Chem. Phys.* **1989**, *91*, 6254.

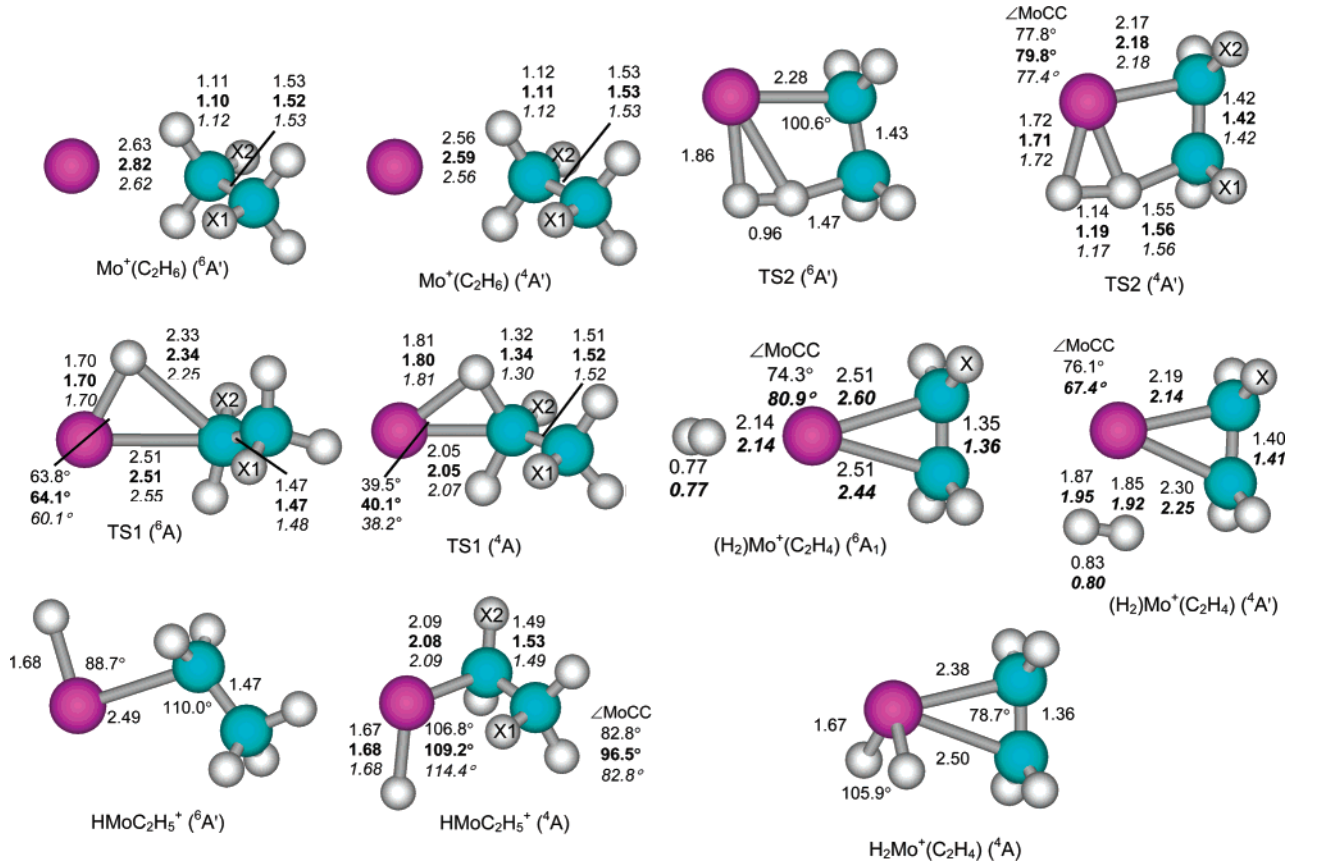

Figure 2. Structures of several intermediates and transition states relevant to CH bond activation along the sextet and quartet surfaces of the $[Mo,2C,6H]^+$ (upper values) and $[Mo,3C,8H]^+$ systems (primary CH bond activation in bold, secondary CH bond activation in italics) calculated at the B3LYP/HW/6-311++G(3df,3p) level of theory. X1 and X2 indicate the location of the methyl group for primary and secondary CH bond activation, respectively, in the propane system. Bond lengths are given in Å.

indicating that both ligands are bound covalently. Low-lying excited states of the $HMoC_2H_5^+$ intermediate were also located and provide some insight into the stability of this complex. The ^4A ground conformer is stabilized by a β-CH agostic interaction with Mo^+, as indicated by a Mo−H distance of 1.93 Å and ∠MoCC = 83°, Figure 2. In contrast, the ^4A excited conformer, which lies 0.36 eV higher in energy, is stabilized by an α-CH agostic interaction, where the Mo−H distance is 2.03 Å and ∠MoCC = 127°. Likewise, the $^6A'$ state shown in Figure 2 is characterized by an ∠HMoCC dihedral angle of 180°, whereas 0.013 eV higher in energy is another $^6A'$ conformer having a dihedral angle of 0°.

The large change in energy between the two spin states upon CH bond activation is also reflected in the character of TS1. The sextet state of TS1 is a late transition state in which the hydrogen atom has moved to Mo with long bonds for MoC and CH, Figure 2. In contrast, the quartet state of TS1 is an early transition state in which the CH bond is just beginning to become extended, Figure 2. Although the crossing seam between the quartet and sextet surfaces was not explicitly located, the relative energetics in this region suggest that it occurs on the entrance side near ^{4}TS1, Figure 1.

Once the $HMoC_2H_5^+$ intermediate is formed, dehydrogenation can then proceed over TS2, a four-centered transition state on both the quartet and sextet surfaces, to directly form the $(H_2)Mo^+(C_2H_4)$ intermediates. The quartet state of TS2 is again much lower in energy than the sextet state, Table 1. TS2 ($^4A'$) has relatively short MoH and MoC bond distances (1.72, 1.74, and 2.17 Å, respectively), whereas these bond lengths in the $^6A'$ state are 1.86, 2.14, and 2.28 Å, respectively. Nevertheless, the $(H_2)Mo^+(C_2H_4)$ intermediates again reverse the state ordering, reflecting the fact that $Mo^+(C_2H_4)$ has a $^6A_1$ ground state. Indeed, the calculated binding energy of H_2 to $Mo^+(C_2H_4)$ ($^6A_1$) is 0.33 eV, only slightly weaker than that to $Mo^+(C_2H_4)$ ($^4B_2$), 0.50 eV. Interestingly, the geometries of the $(H_2)Mo^+(C_2H_4)$ complexes are quite distinct, Figure 2. In the $^6A_1$ state, which has C_{2v} symmetry, the two ligands are located on opposite sides of the molybdenum center, reflecting the fact that both ligands are donating into the same empty 5s-4dσ hybrid orbital. The ligands are located in perpendicular planes, which allows back-bonding interactions with different 4dπ orbitals. Rotation of the H_2 about the symmetry axis leads to a $^6A_1$ transition state (imaginary frequency of 230 cm^{-1}), also having C_{2v} symmetry, in which the planes of the ligands are parallel. This transition state lies only 0.007 eV higher in energy, reflecting the loosely bound H_2. In contrast, the covalent nature of the Mo^+ interaction with ethene in the $^4B_2$ state means that the hydrogen molecule prefers to bind to the side and in the same plane as the ethene molecule, such that this $^4A'$ complex has C_s symmetry. Stable $(H_2)Mo^+(C_2H_4)$ complexes having quartet spin and C_{2v} symmetry were located but lie 0.23 ($^4B_2$), 0.84 ($^4B_1$), 1.06 ($^4A_1$), and 1.68 ($^4A_2$) eV above the $^4A'$ state, Table 1. Several doublet states were also located but lie >1.7 eV above the $^6A_1$ ground state.

An alternative pathway for dehydrogenation could involve transfer of a hydrogen atom from the ethyl ligand of $HMoC_2H_5^+$ to the molybdenum center to form the dihydride, $(H)_2Mo^+(C_2H_4)$. Such an intermediate was located on the quartet surface, but could not be found on the sextet surface, despite repeated efforts. This intermediate has MoH bond lengths of 1.67 Å each and a HMoH bond angle of 106°, indicating that they are both covalent bonds and that this part of the complex is very similar

Table 1. Theoretical Energies of $[Mo,2C,6H]^+$ Intermediates, Transition States, and Products Relevant to CH Bond Activation Calculated at the B3LYP/HW/6-311++G(3df,3p) Level of Theory

species	state	$s(s+1)$[a]	energy (E_h)	ZPE (E_h)[b]	E_{rel} (eV)[c]
$Mo^+ + C_2H_6$	$^6S + {}^1A_{1g}$	8.75 + 0.00	−147.020944	0.074280	0.000
	$^4G + {}^1A_{1g}$	3.75 + 0.00	−146.950227	0.074280	1.924
$MoH_2^+ + C_2H_4$	$^6A_1 + {}^1A_g$	8.75 + 0.00	−146.973893	0.063012	0.977
$MoC_2H_4^+ + H_2$	$^6A_1 + {}^1\Sigma_g^+$	8.76 + 0.00	−147.008428	0.062363	0.020
	$^4B_2 + {}^1\Sigma_g^+$	3.78 + 0.00	−146.989061	0.061747	0.530
$MoC_2H_2^+ + 2H_2$	$^4A_2 + {}^1\Sigma_g^+$	3.78 + 0.00	−146.937598	0.048685	1.579
$MoC_2H_5^+ + H$	$^5A' + {}^2S$	6.04 + 0.75	−146.931637	0.062155	2.104
$MoC_2H_3^+ + H + H_2$	$^5A'' + {}^2S + {}^1\Sigma_g^+$	6.09 + 0.75	−146.847846	0.050510	4.071
$MoC_2H^+ + H + 2H_2$	$^5\Sigma^+ + {}^2S + {}^1\Sigma_g^+$	6.04 + 0.75	−146.794032	0.037532	5.186
$MoH^+ + C_2H_5$	$^5\Sigma^+ + {}^2A'$	6.03 + 0.75	−146.925704	0.063423	2.299
$Mo^+(C_2H_6)$	$^6A'$	8.75	−147.042683	0.074365	−0.589
	$^4A'$	4.75*	−146.998720	0.073951	0.596
	$^4A''$	3.76	−146.987140	0.070614	0.821
	$^2A'$	2.72*	−146.976012	0.074056	1.217
	$^6A''$	8.76	−146.969077	0.073999	1.404
	$^2A''$	1.76*	−146.962542	0.071689	1.519
TS1	^4A	3.76	−146.986882	0.067186 (347)	0.736
	^6A	8.75	−146.975119	0.066782 (478)	1.045
$HMoC_2H_5^+$	^4A	3.79	−147.019013	0.068400	−0.106
	^4A	3.81	−147.004898	0.067372	0.251
	$^6A'$ (180°)[d]	8.78	−146.977847	0.066654	0.967
	$^6A'$ (0°)[d]	8.78	−146.977437	0.066733	0.980
TS2	$^4A'$	3.79	−147.008229	0.066197 (967)	0.129
	$^6A'$	8.78	−146.950351	0.063652 (1147)	1.635
$(H_2)Mo^+(C_2H_4)$	$^6A_1$ (⊥)[e]	8.76	−147.024301	0.066022	−0.314
	$^6A_1$ (||)[e,f]	8.76	−147.023319	0.065268 (230)	−0.307
	$^4A'$	3.78	−147.014669	0.068488	0.015
	$^4B_2$ (||)[e]	3.77	−147.003955	0.066392	0.250
	$^4B_1$ (||)[e]	3.76	−146.981630	0.066453	0.859
	$^4A_1$ (⊥)[e]	3.76	−146.973058	0.065889	1.077
	$^2A_1$ (⊥)[e]	0.75	−146.962906	0.067865	1.407
	$^2A_2$ (⊥)[e]	0.75	−146.962230	0.068045	1.430
	$^2B_1$ (⊥)[e]	1.75*	−146.960074	0.074727	1.668
	$^4A_2$ (⊥)[e]	3.75	−146.951039	0.066654	1.697
TS $[(H)_2Mo^+(C_2H_4)]$[g]	^4A	3.78	−147.000680	0.064175 (305)	0.279
$(H)_2Mo^+(C_2H_4)$	^4A	3.78	−147.001187	0.064697	0.280

[a] Spin contamination marked by asterisks. [b]Zero-point energy. Imaginary frequencies in cm^{-1} are listed in parentheses. [c]Energy relative to the ground state species for each compound including zero-point energies (scaled by 0.989). [d]Angle refers to the HMoCC dihedral angle. [e]Refers to whether the HMoH and CMoC planes are parallel (||) or perpendicular (⊥) to one another. [f]This is the transition state for rotation of the H_2 molecule along the axis binding to Mo. [g]Transition state between $HMoC_2H_5^+$ and $(H)_2Mo^+(C_2H_4)$.

to MoH_2^+ ($^4B_2$), where the geometrical parameters are 1.67 Å and 114°. As a consequence, the Mo−C bond lengths are considerably longer (2.38 and 2.50 Å), Figure 2, compared with $Mo^+(C_2H_4)$ ($^4B_2$), where they are 2.14 Å. Notably, the energy of this intermediate lies above that for TS2 and the transition state for forming this intermediate is nearly isoenergetic with the dihydride intermediate, Table 1. As a consequence, the lowest energy pathway for going from $(H)_2Mo^+(C_2H_4)$ to $(H_2)Mo^+(C_2H_4)$ is to return to $HMoC_2H_5^+$ and then over TS2. Despite repeated efforts, attempts to locate a transition state directly between the $(H)_2Mo^+(C_2H_4)$ and $(H_2)Mo^+(C_2H_4)$ quartet intermediates always collapsed to TS2 ($^4A'$).

Overall, the potential energy surface of Figure 1 agrees nicely with experimental observations. As hypothesized in Paper I from the derived thermochemistry,[1] dehydrogenation of ethane by Mo^+ (^6S) is limited by a barrier in excess of the energy asymptotes for the products. If spin is conserved, then the limiting transition state is TS2 ($^6A'$), calculated to lie 1.64 eV above ground state reactants. This is well above the threshold determined for production of $Mo^+(C_2H_4) + H_2$ of 0.52 ± 0.03 eV.[1] If spin is disregarded, the highest energy point between reactants and products is TS1 (^4A), calculated to lie at 0.74 eV. This is in reasonable agreement with experiment, especially given the comparisons between experiment and the calculations detailed in Paper I (average differences of about 0.3 eV).[1] It might be noted that because TS1 (^4A) lies above both the $^6A_1$ and $^4B_2$ states of $Mo^+(C_2H_4)$, it is feasible that both states can be formed. Depending on the facility with which the transition from the quartet to the sextet surface in the exit channel is made, formation of either $Mo^+(C_2H_4)$ ($^6A_1$), which is energetically favored, or $Mo^+(C_2H_4)$ ($^4B_2$), which need not change spin, could dominate the products. The experiments of Paper I have no means of ascertaining which of these states predominates.[1]

Dehydrogenation of Propane: $Mo^+(C_3H_6) + H_2$ Formation. Because of their complexity, calculations on the potential energy surface for C−H bond activation of propane included only the key reaction intermediates and transition states. Like the ethane system, we expect that the rate-limiting transition state for dehydrogenation of propane should be TS1 on the quartet surface. This is consistent with the very similar threshold energies observed experimentally for dehydrogenation of ethane, 0.52 ± 0.03 eV, and propane, 0.41 ± 0.05 eV.[1] Certainly, it is reasonable that substituting a methyl group for one of the hydrogens will not perturb the system extensively; however, such substitution allows surfaces corresponding to both primary and secondary C−H bond activation. Detailed calculations confirm these general expectations, as shown in the potential energy surfaces of Figure 3. Structures of these species are shown in Figure 2, and Table S2 in the Supporting Information provides more complete structural information.

Calculations indicate that there are two stable minima for the $Mo^+(C_3H_8)$ complex on both the sextet and quartet spin surfaces, Table 2. When the metal ion associates near the secondary carbon to form $Mo^+(2\text{-}C_3H_8)$, the complexes have geometries very similar to those for ethane, as shown in Figure 2. Both sextet and quartet complexes have C_{2v} symmetry, although the quartet complex exhibits an imaginary frequency such that a slightly distorted complex lies 0.002 eV lower in energy before zero-point energy considerations, but 0.044 eV higher after. Alternatively, the metal ion can associate on the other side of the propane molecule, forming $Mo^+(1\text{-}C_3H_8)$. The sextet spin state has C_{2v} symmetry such that there are two equal Mo−C bond lengths of 2.82 Å that are extended compared to the Mo−C bond lengths in $Mo^+(C_2H_6)$ and $Mo^+(2\text{-}C_3H_8)$, 2.63 and 2.62 Å, respectively, Figure 2. In the quartet spin analogue, the metal ion shifts closer to one of the primary carbons such that the Mo−C bond length is only slightly longer than the $Mo^+(C_2H_6)$ and $Mo^+(2\text{-}C_3H_8)$ analogues, 2.59 vs 2.56 and 2.56 Å, respectively, Figure 2. The $Mo^+(1\text{-}C_3H_8)$ ($^6A_1$) state lies 0.05 eV lower in energy than $Mo^+(2\text{-}C_3H_8)$ ($^6A_1$) and is 0.13 eV more strongly bound than $Mo^+(C_2H_6)$ ($^6A'$). On the quartet surface, the two $Mo^+(C_3H_8)$ complexes are nearly isoenergetic, Table 2, and about 0.1 eV more strongly bound than the analogous $Mo^+(C_2H_6)$ ($^4A'$) complex.

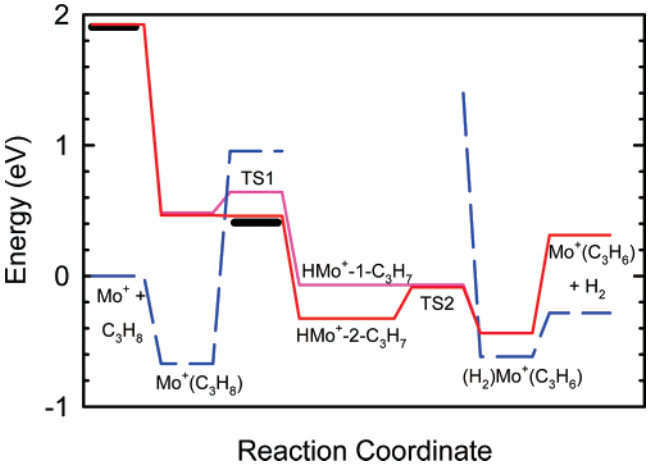

Figure 3. $[Mo,3C,8H]^+$ potential energy surfaces for CH bond activation derived from theoretical results. Sextet spin surfaces are indicated by the blue dashed line and quartet spin surfaces by the red and pink full lines. The energies of all species relative to the Mo^+ (^6S) + C_3H_8 ground state asymptote are based on ab initio calculations (B3LYP/HW/6-311++G(3df,3p), see Table 2). Heavy horizontal lines indicate experimentally measured values.

Identification of TS1 on the quartet surface for activation of a primary C−H bond, ^{4}TS1(1), shows a geometry very similar to that for C−H bond activation in ethane, Figure 2. The imaginary frequency of 409 cm^{-1} corresponds primarily to motion of the hydrogen atom being transferred. The energy of this transition state is 0.64 eV above the ground state reactants, which is 0.09 eV lower than ^{4}TS1 in the ethane system. This difference is comparable to the difference in activation energies observed experimentally between ethane and propane, 0.11 ± 0.06 eV. On the sextet surface, ^{6}TS1(1) was found to lie 0.96 eV above the ground state reactants, 0.31 eV above ^{4}TS1(1), a difference nearly identical to the results for $Mo^+(C_2H_6)$, where ^{6}TS1 lies 0.31 eV above ^{4}TS1, Table 1. The imaginary frequency of 457 cm^{-1} again correspond to H atom motion, whereas the geometry shows that this transition state is later than that on the quartet surface.

One anticipates that secondary C−H bond activation may be slightly favored because this bond is weaker than the primary C−H bond by 0.05 ± 0.03 eV; however, the deeper well for $Mo^+(1\text{-}C_3H_8)$ may mediate this preference. Unfortunately, location of the comparable transition state for secondary C−H bond activation, ^{4}TS1(2), was more problematic. When a geometry optimization was begun with an appropriate geometry based on TS1 from $Mo^+(C_2H_6)$ or $Mo^+(1\text{-}C_3H_8)$, the energy rapidly dropped to about 0.46 ± 0.03 eV above ground state reactants, Table 2, but convergence always led to an even lower energy transition state at 0.30 eV. The imaginary frequency in this transition state (839 cm^{-1}) corresponds to an exchange of the hydrogen on Mo^+ with the other secondary hydrogen; hence this transition state is not TS1. Nevertheless, the energies of ^{4}TS1(1) at 0.64 eV and the estimate for ^{4}TS1(2) at 0.46 ± 0.03

Table 2. Theoretical Energies of $[Mo,3C,8H]^+$ Intermediates, Transition States, and Products Relevant to CH Bond Activation Calculated at the B3LYP/HW/6-311++G(3df,3p) Level of Theory

species	state	$s(s+1)$[a]	energy (E_h)	ZPE (E_h)[b]	E_{rel} (eV)[c]
$Mo^+ + C_3H_8$	$^6S + {}^1A_1$	8.75 + 0.00	−186.347808	0.102808	0.000
$MoH_2^+ + C_3H_6$	$^6A_1 + {}^1A$	8.75 + 0.00	−186.306369	0.091487	0.823
$MoC_3H_6^+ + H_2$	$^6A + {}^1\Sigma_g^+$	8.76 + 0.00	−186.346037	0.090489	−0.283
	$^4A + {}^1\Sigma_g^+$	3.86 + 0.00	−186.323271	0.089646	0.313
$MoH^+ + 1\text{-}C_3H_7$	$^5\Sigma^+ + {}^2A$	6.03 + 0.75	−118.516574	0.092153	2.311
$MoH^+ + 2\text{-}C_3H_7$	$^5\Sigma^+ + {}^2A'$	6.03 + 0.75	−186.258551	0.091809	2.133
$MoH + 1\text{-}C_3H_7^+$	$^6\Sigma^+ + {}^1A$	8.76 + 0.00	−186.237433	0.091273	2.693
$MoH + 2\text{-}C_3H_7^+$	$^6\Sigma^+ + {}^1A_1$	8.76 + 0.00	−186.270754	0.091440	1.791
$Mo^+(1\text{-}C_3H_8)$	$^6A_1$ (C_{2v})[d]	8.75	−186.373680	0.102233	−0.717
	$^4A'$ (C_s)[d]	4.75*	−186.329088	0.101877	0.484
	$^4A''$ (C_s)[d]	3.76	−186.317324	0.099093	0.730
$Mo^+(2\text{-}C_3H_8)$	$^6A_1$ (C_{2v})[d]	8.75	−186.372180	0.102573	−0.670
	^4A (C_1)[d]	4.74*	−186.328639	0.102355	0.509
	$^4A_2$ (C_{2v})[d]	4.75*	−186.328573	0.100636 (199)	0.465
	$^4A_2$ (C_{2v})[d]	3.76	−186.300421	0.102142	1.272
TS1(1)	^4A	3.76	−186.316937	0.095448 (409)	0.642
	^6A	8.78	−186.304998	0.095033 (457)	0.956
TS1(2) estimate[e]	^4A	3.77	−186.321(1)		0.46(3)
	^6A	8.78	−186.314166	0.095184 (512)	0.710
$HMo^+-1\text{-}C_3H_7$	^4A	3.79	−186.344460	0.096850	−0.069
$HMo^+-2\text{-}C_3H_7$	^4A	3.79	−186.353259	0.096227	−0.325
TS(2) exchange[f]	^4A	3.77	−186.326635	0.092687 (839)	0.304
TS2(1)	^4A	3.79	−186.341532	0.093951 (893)	−0.068
TS2(2)	^4A	3.79	−186.342158	0.093872 (994)	−0.087
$(H_2)Mo^+(C_3H_6)$	^6A	8.76	−186.361840	0.094082	−0.617
	^4A	3.78	−186.355496	0.094348	−0.437
	^4A	3.77	−186.338280	0.095508	0.063

[a] Spin contamination marked by asterisks. [b]Zero-point energies. Imaginary frequencies are listed in parentheses in units of cm^{-1}. [c]Energy relative to the ground state species for each compound including zero-point energies (scaled by 0.989). [d]Symmetry designation of this complex. [e]This transition state converges to TS(2) exchange. The estimated energy is obtained as described in the text. [f]This transition state exchanges the two secondary hydrogens on $H-Mo^+-2\text{-}C_3H_7$.

eV are in qualitative agreement with the observed threshold for dehydrogenation in the propane system, 0.41 ± 0.05 eV,[1] Figure 3.

Continuing along the quartet surface, one finds both HMo^+-1-C_3H_7 and HMo^+-2-C_3H_7 intermediates, which lie 0.07 and 0.32 eV, respectively, lower in energy than the ground state reactants. The former energy is similar to that for $HMo^+C_2H_5$, 0.11 eV lower than reactants. Geometries of these three complexes are similar, Figure 2, with the most notable difference being the MoCC bond angle for HMo^+-1-C_3H_7. This is determined largely by an agostic interaction between the terminal methyl group and the molybdenum ion, which also explains why the CC bond length increases from 1.49 Å to 1.53 Å, Figure 2. Activation of a β-H in both complexes leads to TS2(1) and TS2(2), which have very similar geometries to TS2 in the ethane system, Figure 2. The energies are comparable, 0.07 and 0.09 eV, respectively, below the ground state reactants, compared with 0.13 eV above in the ethane system. Clearly, the longer hydrocarbon chain leads to stabilization of all the intermediates and transition states along the potential energy surface.

Both TS2(1) and TS2(2) lead to formation of the $(H_2)Mo^+$-(C_3H_6) (^4A) complex, which lies 0.44 eV below the reactants. As in the ethane system, the sextet analogue is lower in energy, here by 0.18 eV, Table 2, compared to a difference of 0.33 eV in the ethane system. In the quartet state, the geometry of $(H_2)Mo^+(C_3H_6)$ differs somewhat from that of $(H_2)Mo^+(C_2H_4)$ mainly in that the MoC bond lengths are shorter (by about 0.05

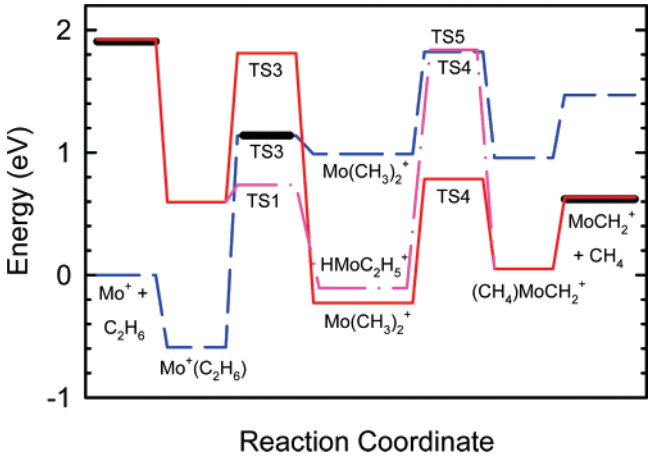

Figure 4. $[Mo,2C,6H]^+$ potential energy surfaces for CC bond activation derived from theoretical results. Sextet spin surfaces are indicated by the blue dashed line and quartet spin surfaces by the red full line and pink dash-dot line. The energies of all species relative to the Mo^+ (^6S) + C_2H_6 ground state asymptote are based on ab initio calculations (B3LYP/HW/6-311++G(3df,3p), see Table 3). Heavy horizontal lines indicate experimentally measured values.

Å), leading to longer MoH bond lengths (by about 0.07 Å). This is clearly a result of the stronger binding of propene compared to ethene. There is less distortion in the sextet analogues, Figure 2. From these complexes, dihydrogen loss is straightforward, yielding the ^6A ground and ^4A excited states of $Mo^+(C_3H_6)$. The dihydrogen binding energies are 0.33 and 0.75 eV, respectively, in reasonable accord with the values for the analogous ethene complexes, 0.33 and 0.52 eV, respectively.

Overall, the potential energy surface in Figure 3 is consistent with experimental observations. Dehydrogenation of propane is limited by ^{4}TS1, such that this exothermic process exhibits a barrier. Both primary and secondary CH bond activation may be involved, with the latter being favored by about 0.2 eV. Because ^{4}TS1 lies above both the sextet and quartet states of $Mo^+(C_3H_6)$ + H_2, both states can plausibly be formed in the experiments.

C−C Bond Activation in Ethane: $MoCH_2^+$ + CH_4 Formation. The low-energy C−C bond activation process observed for ethane is formation of $MoCH_2^+$ + CH_4, Figure 1b in Paper I.[1] This reaction is likely to follow the same type of mechanism as the formation of $MoCH_2^+$ in the methane system:[3] specifically, elimination of RH from H−Mo^+−CH_2−R or H_3C−Mo^+−R intermediates (R = H for methane and CH_3 for ethane), both passing through four-center transition states. The ethane reaction is less efficient (maximum cross section of 2×10^{-17} cm^2) than the reaction in the methane system (maximum cross section of 7×10^{-17} cm^2) because there is no competition with other more favorable reactions in the latter system and the four-center transition state is probably more restricted when an alkyl group rather than an H atom is involved as R.

Results of our calculations of the methane elimination pathway for the ethane reaction system are shown in Figure 4. Figure 5 shows the structures of the intermediates and transition states located on both the sextet and quartet surfaces for C−C bond activation, and Table S3 in the Supporting Information provides more complete structural information. As for C−H bond activation, the reaction starts by forming the $Mo^+(C_2H_6)$ intermediate. After passing over TS3, the next intermediate formed is the molybdenum dimethyl cation, $Mo(CH_3)_2^+$, where the quartet species lies much lower in energy than the sextet species. Again this is because the formation of two covalent

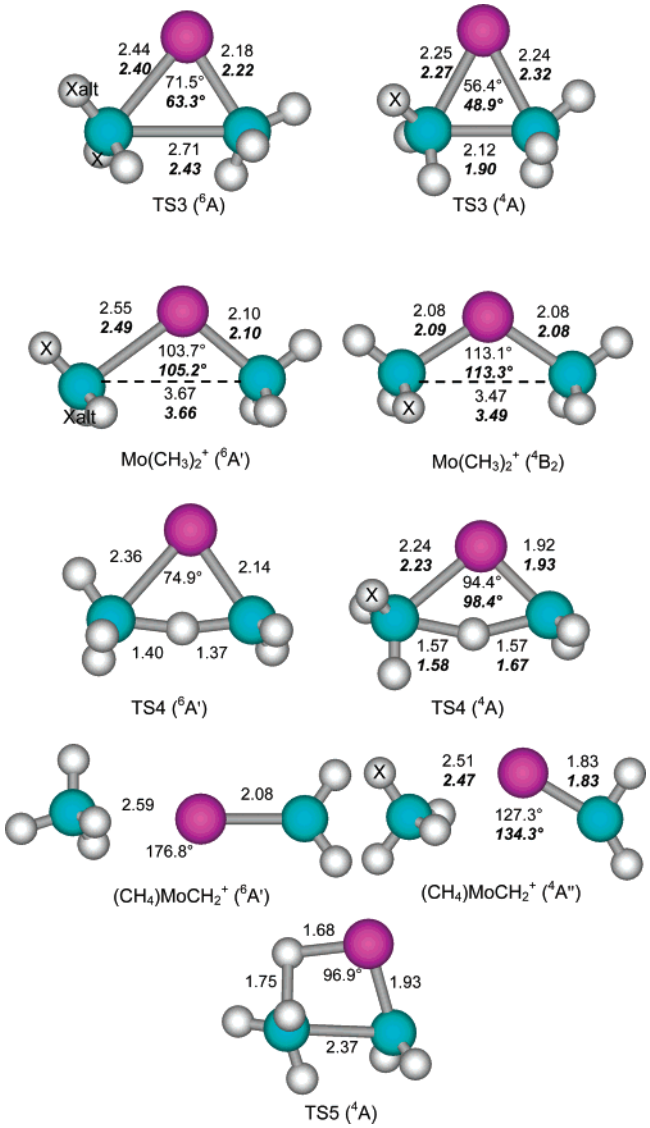

Figure 5. Structures of several intermediates and transition states relevant to CC bond activation leading to $MoCH_2^+$ along the sextet and quartet surfaces of the $[Mo,2C,6H]^+$ (upper values) and $[Mo,3C,8H]^+$ systems (bold values) calculated at the B3LYP/HW/6-311++G(3df,3p) level of theory. X indicates the location of the methyl group in the propane system. Bond lengths are given in Å.

bonds to Mo^+ necessitates the quartet spin. This is evidenced by the fact that the $^4B_2$ ground state of $Mo(CH_3)_2^+$ has C_{2v} symmetry, with equal Mo−C bond lengths of 2.08 Å, similar to the covalent single bond in $MoCH_3^+$, 2.10 Å.[1] In contrast, on the sextet surface, the $^6A'$ state of $Mo(CH_3)_2^+$ has one Mo−C bond length of 2.10 Å, indicating a covalent single bond, but the second Mo−C bond length is 2.55 Å, consistent with a bond order of only 1/2. Our results for $Mo(CH_3)_2^+$ are in reasonable agreement with those previously obtained by Rosi et al.[41] They obtained a $^4B_2$ ground state with Mo−C bond lengths of 2.09 Å and bond angles for CMoC of 115° and MoCH of 108°, compared with our values of 2.08 Å, 113°, and 108°, respectively. However, they calculate that the loss of both methyl groups from this molecule costs 2.93 eV (empirically adjusted to 3.45 eV), whereas our calculations indicate the sum of these bond energies is 3.80 eV. Both of these values are about 0.3 eV stronger than twice the Mo^+−CH_3 bond energy calculated at the same level, 1.76 eV for the present results and 1.31 eV (empirically adjusted to 1.57 eV) from Rosi et al. The key distinction that this difference in energies makes is whether the

Table 3. Theoretical Energies of $[Mo,2C,6H]^+$ Intermediates, Transition States, and Products Relevant to CC Bond Activation Calculated at the B3LYP/HW/6-311++G(3df,3p) Level of Theory

species	state	$s(s+1)$[a]	energy (E_h)	ZPE (E_h)[b]	E_{rel} (eV)[c]
$Mo^+ + C_2H_6$	$^6S + {}^1A_{1g}$	8.75 + 0.00	−147.020944	0.074280	0.000
$MoCH_2^+ + CH_4$	$^4B_1 + {}^1A_1$	3.93 + 0.00	−146.988667	0.065172	0.633
	$^6A_1 + {}^1A_1$	8.76 + 0.00	−146.958405	0.065771	1.473
$MoCH_3^+ + CH_3$	$^5A_1 + {}^2A_2''$	6.05 + 0.75	−146.943453	0.062778	1.799
$MoCH^+ + CH_3 + H_2$	$^3\Sigma^- + {}^2A_2'' + {}^1\Sigma_g^+$	2.10 + 0.75	−146.873262	0.051751	3.412
TS3	^6A	8.79	−146.972871	0.067958 (228)	1.138
	^4A	4.69*	−146.949689	0.069530 (422)	1.811
$Mo(CH_3)_2^+$	$^4B_2$ (C_{2v})[d]	3.79	−147.022812	0.067698	−0.228
	$^4A_2$ (C_{2v})[d]	3.77	−147.002704	0.071623	0.425
	$^6A'$ (C_s)[d]	8.79	−146.976918	0.066458	0.988
	$^6A_1$ (C_{3v})[d]	8.77	−146.967625	0.066023	1.229
	$^6A_2''$ (D_{3h})[d]	8.75	−146.966273	0.066773 (239)[e]	1.286
	$^6A_2$ (C_{2v})[d]	8.75	−146.930438	0.070649	2.365
TS4	^4A	3.83	−146.983063	0.065154 (1293)[f]	0.786
	^6A	8.75	−146.943415	0.063586 (1067)[f]	1.822
$(CH_4)MoCH_2^+$	$^4A''$	3.86	−147.011823	0.066927	0.050
	$^2A''$	1.75*	−146.988439	0.067008	0.689
	$^6A'$	8.76	−146.979226	0.067667	0.957
	^2A	0.78	−146.970941	0.065704	1.130
	$^4A'$	3.94	−146.962268	0.066792	1.395
	$^6A''$	8.76	−146.954516	0.068340	1.648
TS5	^4A	3.80	−146.944840	0.065610 (926)	1.838

[a] Spin contamination marked by asterisks. [b] Zero point energy. Imaginary frequencies in cm^{-1} are listed in parentheses. [c] Energy relative to the ground state species for each compound including zero-point energies (scaled by 0.989). [d] Symmetry designation of this complex. [e] This imaginary motion corresponds to an asymmetric C−Mo−C stretch. [f] More symmetric (C_s) versions of these transition states have additional imaginary frequencies of 16 cm^{-1} ($^4A'$) and 54 cm^{-1} ($^6A'$) corresponding to a methyl torsion.

$Mo(CH_3)_2^+$ complex is stable with respect to dissociation to $Mo^+ + C_2H_6$. Our results indicate the complex lies 0.23 eV below the ground state reactants, whereas the thermochemistry of Rosi et al. suggests it lies 0.4−1.0 eV above.[41]

A comparison of the energies of the $Mo(CH_3)_2^+$ intermediates with those of $HMoC_2H_5^+$ shows that they are similar, −0.23 and −0.11 eV, respectively, relative to ground state reactants on the quartet surface and 0.99 and 0.97 eV, respectively, on the sextet surface. Excited states of the $Mo(CH_3)_2^+$ intermediate were also located and include $^4A_2$ (C_{2v} symmetry), $^6A'$ (C_s), $^6A_1$ (C_{3v}), $^6A_2''$ (D_{3h}), and $^6A_2$ (C_{2v}), with energies listed in Table 3.

Similar to the energies of the intermediates, the energies of the transition states leading to these intermediates, TS3 and TS1, are comparable on the sextet surface, 1.14 and 1.04 eV, respectively. In contrast, the energies of these transition states on the quartet surface differ appreciably, 1.81 and 0.74 eV, respectively. Comparison of the structures of these transition states shows that the two sextet species are roughly similar (Figures 2 and 5), whereas in the quartet species, the C−C bond activation leads to much longer Mo−C bonds in TS3 (2.24 and 2.25 Å) than the Mo−H and Mo−C bonds in TS1 (1.81 and 2.05 Å, respectively). Presumably, the directionality of the sp^3 orbital of CH_3 compared to the spherical 1s orbital on H induces this difference in transition state energies. On the sextet surface, this is mediated by the fact that a covalent bond is not being formed to one of the fragments. We also note that the Mo−C bond lengths of TS3 are not symmetric for either the quartet or sextet state, because the hydrogen atoms on the methyl groups still want to remain staggered with respect to one another, Figure 5. Although the crossing seam between the quartet and sextet surfaces was not explicitly located, the relative energetics in this region suggest that it occurs on the exit side near ^{6}TS3, Figure 4, in contrast with the situation for C−H bond activation, Figure 1.

Once the dimethyl intermediate is formed, hydrogen migration from one carbon center to the other can occur through a four-centered transition state, TS4, on either the quartet or sextet surface. As might be anticipated, the energy of this transition state is much lower on the quartet surface (by 1.04 eV). Hydrogen migration yields the $(CH_4)MoCH_2^+$ intermediates, which correspond to an intact methane molecule bound to

$MoCH_2^+$. On the sextet surface, this $^6A'$ intermediate has the two ligands located approximately on opposite sides of the metal ion and the $MoCH_2^+$ fragment is largely undistorted from the $MoCH_2^+$ ($^6A_1$) product, Figure 5. In contrast, on the quartet surface, the $^4A''$ $(CH_4)MoCH_2^+$ intermediate distorts the $MoCH_2^+$ ($^4B_1$) product ion, which has C_{2v} symmetry, because the methane molecule is placed to the side of the Mo−C bond. This occurs because the empty orbital in this state is a 5s-4d hybrid orbital that lies perpendicular to the Mo−C bond axis. The energies necessary to lose methane from the $(CH_4)MoCH_2^+$ intermediates are comparable, 0.51 eV on the sextet surface and 0.58 eV on the quartet surface. Several excited states of the $(CH_4)MoCH_2^+$ intermediate were located, Table 3, but the lowest of these, $^2A''$, is heavily spin contaminated and may be an artifact.

It is also conceivable that methane elimination from ethane occurs by forming $HMoC_2H_5^+$ and then using a four-centered transition state to yield the $(CH_4)MoCH_2^+$ intermediate. The transition state for this process, TS5, was located but lies 1.84 eV above the reactant asymptote, Table 3, well above the experimentally determined threshold for $MoCH_2^+ + CH_4$ formation. The primary difficulty with this transition state is the need for the methyl group to simultaneously bind to both the CH_2 group it is leaving and the H atom it is joining. Because of the directionality of the sp^3 hybrid orbital of CH_3, this necessitates long C−C (2.37 Å) and C−H (1.75 Å) bonds, Figure 5. Previous calculations have also found that β-alkyl migrations are higher energy pathways than β-H shifts.[13]

Overall the potential energy surface of Figure 4 shows that there is no pathway for elimination of methane from ethane that does not pass over a transition state lying above the product energy asymptote. From ground state reactants, TS4 ($^6A'$) is the limiting transition state on the sextet surface, whereas if the system crosses to the quartet surface, then TS3 (^6A) is the limiting transition state. The threshold for production of $MoCH_2^+ + CH_4$ (Paper I)[1] has a measured threshold energy of 1.14 ± 0.13 eV, which corresponds nicely to the calculated energy of TS3 (^6A), 1.14 eV. Although ^{4}TS1 is even lower in energy, the $HMo^+-C_2H_5$ intermediate decomposes preferentially by dehydrogenation via ^{4}TS2, rather than the high-energy ^{4}TS5 to give methane loss.

C−C Bond Activation in Propane: $MoCH_2^+ + C_2H_6$ Formation. Two types of low-energy C−C bond alkane elimination processes are observed for propane, formation of $MoCH_2^+ + C_2H_6$ and $Mo^+(C_2H_4) + CH_4$. It seems likely that the mechanism for formation of $MoCH_2^+ + C_2H_6$ in the propane reaction parallels that for the elimination of methane in the ethane system. Substituting a methyl group for a hydrogen atom along the surfaces shown in Figure 4 should not perturb them greatly, such that the analogue to ^{6}TS3 is anticipated to be the rate-limiting transition state for this process. Indeed, calculations of this transition state find that it lies 0.89 eV above ground state reactants, Table 4, in good agreement with the rough threshold of ~1.0 eV measured for this process in Paper I,[1] Figure 6. The quartet version of this TS lies much higher in energy, by 0.62 eV, comparable to the difference of 0.67 eV for analogous species in the ethane system. The geometries of these transition states are similar to TS3 in the ethane system, Figure 5, except that the CC bond distances are shorter, suggesting somewhat earlier transition states resulting from the stronger interaction of Mo^+ with the longer chain hydrocarbon. (Table S4 in the Supporting Information provides more complete structural information.) An alternate sextet transition state, TS3 (^6A alt), was also found when the methyl group lies approximately in the MoCC plane, but lies 0.13 eV higher in energy. In addition, the analogue of the TS(2) exchange transition state described above was located. This transition state lies between the $CH_3-Mo^+-C_2H_5$ and $H-Mo^+-2\text{-}C_3H_7$ intermediates, exchanging the hydrogen and methyl groups with an imaginary frequency of 526 cm^{-1}.

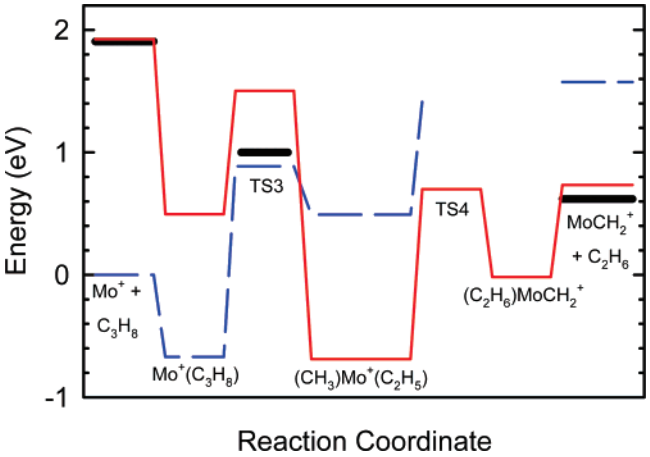

Figure 6. $[Mo,3C,8H]^+$ potential energy surfaces for CC bond activation leading to $MoCH_2^+ + C_2H_6$ derived from theoretical results. Sextet spin surfaces are indicated by the blue dashed line and quartet spin surfaces by the red full line. The energies of all species relative to the Mo^+ (^6S) + C_3H_8 ground state asymptote are based on ab initio calculations (B3LYP/HW/6-311++G(3df,-3p), see Table 4). Heavy horizontal lines indicate experimentally measured values.

Once past ^{6}TS3, the reaction forms the $CH_3-Mo^+-C_2H_5$ intermediate. On the sextet surface, this species lies 0.49 eV above the ground state reactants, whereas the quartet intermediate is again much more stable, lying 0.69 eV below the reactants energy. Both complexes have geometries similar to the $Mo(CH_3)_2^+$ ($^6A'$) and ($^4B_2$) analogues, Figure 5. An alternate geometry for this intermediate on the sextet surface was also located in which the ethyl group is in a gauche rather than trans position relative to the methyl group attached to molybdenum, Figure 5. This conformation lies 0.01 eV higher in energy and has a similar geometry (CC bond length of 3.70 Å), Table S4.

In the ethane system, the sextet surface for forming $MoCH_2^+ + CH_4$ products was high in energy, and therefore the analogous species were not included in the calculations for the propane analogues. On the quartet surface, TS4, the four-centered transition state transferring a methyl H atom to the ethyl group, lies 0.70 eV higher in energy than the ground state reactants. The geometry is similar to the ethane analogue, Figure 5, although now the bridging hydrogen is less symmetrically oriented. This transition state leads directly to the (C_2H_6)-$MoCH_2^+$ intermediate, which lies 0.02 eV below the ground state reactants and 0.75 eV below the $MoCH_2^+$ ($^4B_1$) + C_2H_6 ($^1A_{1g}$) product asymptote. Thus, ethane binds to $MoCH_2^+$ more tightly than methane by 0.17 eV. The geometries of the (C_2H_6)-$MoCH_2^+$ and $(CH_4)MoCH_2^+$ intermediates are comparable, Figure 5, except that the Mo^+-alkane bond distance decreases slightly for the more tightly bound ethane.

Overall, because ^{4}TS4 lies 0.19 eV below the calculated energy of ^{6}TS3, the latter transition state is found to be the rate-limiting step, in agreement with the analogous ethane results. As noted above, the calculated energy of ^{6}TS3 agrees with the rough experimental threshold. The pathway involving ethyl transfer from HMo^+-1-C_3H_7, the analogue of TS5 in the ethane system, was not investigated given the very high energy found for this path in the ethane system.

Table 4. Theoretical Energies of $[Mo,3C,8H]^+$ Intermediates, Transition States, and Products Relevant to CC Bond Activation Calculated at the B3LYP/HW/6-311++G(3df,3p) Level of Theory

species	state	$s(s+1)$[a]	energy (E_h)	ZPE (E_h)[b]	E_{rel} (eV)[c]
$Mo^+ + C_3H_8$	$^6S + {}^1A_1$	8.75 + 0.00	−186.347808	0.102808	0.000
$MoC_2H_4^+ + CH_4$	$^6A_1 + {}^1A_1$	8.76 + 0.00	−186.364925	0.096935	−0.624
	$^4B_2 + {}^1A_1$	3.78 + 0.00	−186.345558	0.096319	−0.113
$MoCH_2^+ + C_2H_6$	$^4B_1 + {}^1A_{1g}$	3.93 + 0.00	−186.313519	0.095417	0.734
	$^6A_1 + {}^1A_{1g}$	8.76 + 0.00	−186.283257	0.096016	1.574
$MoC_2H_5^+ + CH_3$	$^5A' + {}^2A_2''$	6.04 + 0.75	−186.287053	0.091845	1.358
$MoCH_3^+ + C_2H_5$	$^5A_1 + {}^2A'$	6.05 + 0.75	−186.275741	0.092386	1.680
TS3	^6A	8.79	−186.310412	0.097971 (245)	0.887
	^6A (alt)	8.79	−186.303819	0.096065 (219)	1.016
	^4A	3.77	−186.288678	0.098861 (624)	1.503
$(CH_3)Mo(C_2H_5)^+$	^4A	3.79	−186.367100	0.096762	−0.688
	$^6A'$	8.78	−186.322474	0.095471	0.492
	^6A (alt)	8.78	−186.322089	0.095539	0.504
TS exchange[d]	^4A	3.77	−186.316933	0.094215 (526)	0.609
TS4	^4A	3.82	−186.313295	0.093906 (1226)	0.700
$(C_2H_6)MoCH_2^+$	$^4A''$	3.86	−186.342020	0.096287	−0.018
TS6	^4A	3.79	−186.341390	0.094982 (1220)	−0.036
	^6A	8.81	−186.284776	0.091529 (1128)	1.412
$(CH_4)Mo^+(C_2H_4)$	$^6A'$	8.76	−186.384776	0.098271	−1.128
	$^4B_2$	3.78	−186.361492	0.097190	−0.523
TS7	^4A	3.78	−186.324796	0.094715 (382)	0.408
$(CH_3)(H)Mo^+(C_2H_4)$	^4A	3.78	−186.352467	0.093019	−0.390
TS8 estimate[e]	^4A	3.78	−186.32108	0.092887 (1130)	0.460

[a] Spin contamination is indicated by an asterisk. [b] Zero-point energies. Imaginary frequencies in cm^{-1} are listed in parentheses. [c] Energy relative to the ground state species for each compound including zero-point energies (scaled by 0.989). [d] This transition state exchanges the methyl group on $(CH_3)Mo(C_2H_5)^+$ with an α-H to form $H-Mo^+-2\text{-}C_3H_7$. [e] This transition state collapses to TS6. The estimated energy is obtained as described in the text.

C−C Bond Activation in Propane: $Mo^+(C_2H_4) + CH_4$ Formation. The formation of $Mo^+(C_2H_4) + CH_4$ in the propane system is interesting as this C−C bond activation process can be fairly efficient for many metal cations,[34] in particular, the late first-row transition metal cations. In analogy with the dehydrogenation process, it seems likely that this reaction occurs by initial C−C bond activation to form $H_3C-Mo^+-C_2H_5$, followed by a four-centered transition state, TS6, to yield the $(CH_4)Mo^+(C_2H_4)$ intermediate, which then eliminates methane. The calculated surface for this sequence is shown in Figure 7 and is the same as Figure 6 up to the $H_3C-Mo^+-C_2H_5$ intermediate. Calculations located ^{4}TS6 and find that it lies 0.04 eV below the energy of the reactants. Thus, this pathway is calculated to be limited by the initial C−C bond activation process, namely, ^{6}TS3, which is found to lie 0.89 eV above the reactants. This value is in reasonable agreement with the experimentally measured threshold for this process of 0.75 ± 0.12 eV (Paper I).[1] The geometry of ^{4}TS6 is shown in Figure 8. (Table S4 in the Supporting Information provides more complete structural information.) It can be seen that the β-H on the ethyl group is being transferred to the methyl group on molybdenum while interacting with the metal ion. The imaginary frequency of 1120 cm^{-1} corresponds almost exclusively to hydrogen motion between the two carbon centers. This multicenter transition state has a geometry similar to that of ^{4}TS4, Figure 5, with MoC and CC bond lengths comparable to those in the $(CH_4)Mo^+(C_2H_4)$ ($^4B_2$) intermediate, Figure 8. In this intermediate, the $Mo^+(C_2H_4)$ part of the molecule is only slightly distorted from that of the $^4B_2$ ground state product (see Figure 3 in Paper I).[1] Likewise the sextet intermediate has a geometry similar to the $^6A_1$ state of $Mo^+(C_2H_4)$ with a methane molecule loosely bound on the opposite side of the metal ion. As shown in Figure 8, the sextet state of TS6 has a methyl group that is nearly completely detached from the metal ion in order to interact with the transferring hydrogen. This is consistent with the fact that the energy of this geometry, 1.41 eV, lies near the calculated energy of the $MoC_2H_5^+ + CH_3$ product asymptote at 1.36 eV, Table 4.

If ^{6}TS3 is indeed the limiting transition state for $Mo^+(C_2H_4) + CH_4$, then it should have the same threshold energy as

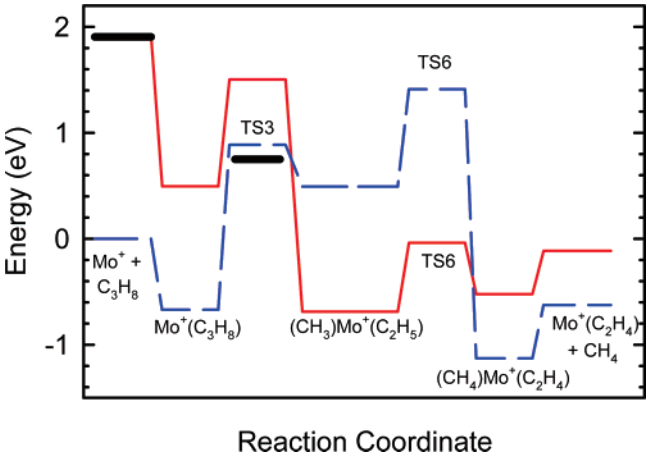

Figure 7. $[Mo,3C,8H]^+$ potential energy surfaces for CC bond activation leading to $Mo^+(C_2H_4) + CH_4$ derived from theoretical results. Sextet spin surfaces are indicated by the blue dashed line and quartet spin surfaces by the red full line. The energies of all species relative to the Mo^+ (^6S) + C_3H_8 ground state asymptote are based on ab initio calculations (B3LYP/HW/6-311++G(3df,-3p), see Table 4). Heavy horizontal lines indicate experimentally measured values.

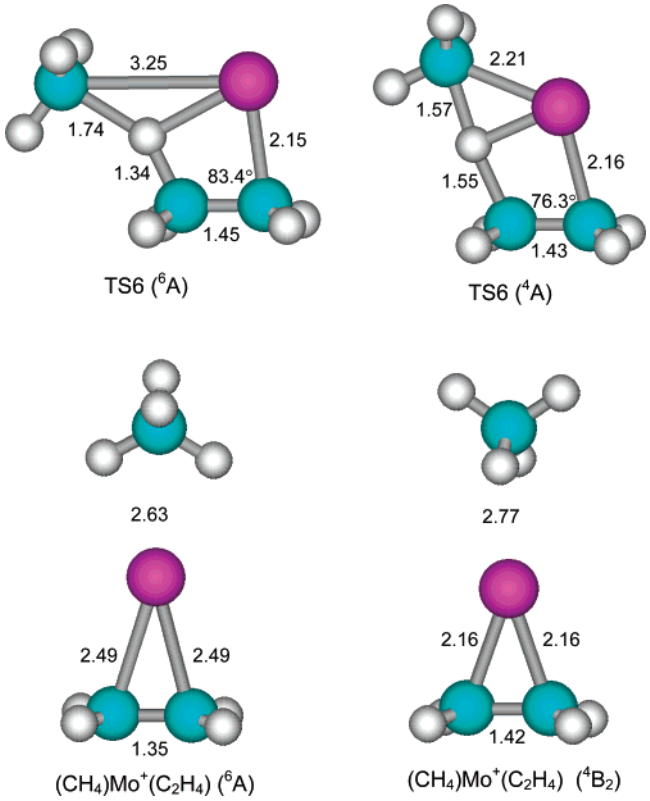

Figure 8. Structures of several intermediates and transition states relevant to CC bond activation leading to $Mo^+(C_2H_4)$ along the sextet and quartet surfaces of the $[Mo,3C,8H]^+$ system calculated at the B3LYP/HW/6-311++G(3df,3p) level of theory. Bond lengths are given in Å.

formation of $MoCH_2^+ + C_2H_6$, which is also limited by ^{6}TS3. This is approximately correct, as the former reaction has an E_0 of 0.75 ± 0.12 eV and the latter reaction has an estimated threshold of ~1.0 ± 0.2 eV.[1] Competition between these two channels is controlled by the relative energies of ^{4}TS6 at −0.04 eV (Figure 7) and ^{4}TS4 at 0.79 eV (Figure 6), respectively. This is consistent with the observation that the former channel is about 30 times larger than the latter process, Figure 2 in Paper I.[1] This competition may also explain why the apparent barrier for loss of ethane is somewhat higher than that measured for loss of methane; that is, there is a competitive shift.

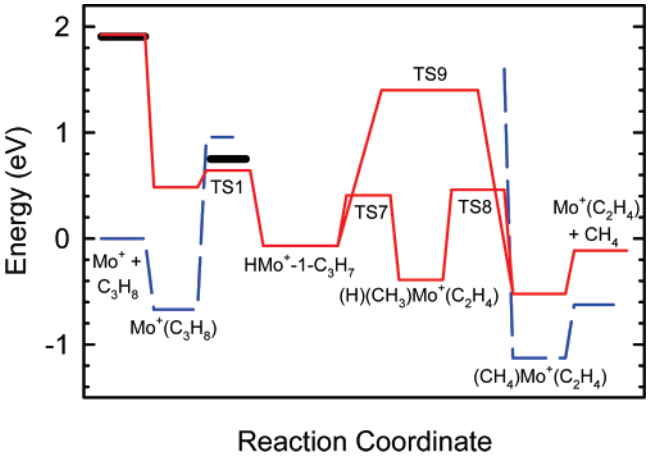

Figure 9. $[Mo,3C,8H]^+$ potential energy surfaces for CH bond activation leading to $Mo^+(C_2H_4) + CH_4$ derived from theoretical results. Sextet spin surfaces are indicated by the blue dashed line and quartet spin surfaces by the red full line. The energies of all species relative to the Mo^+ (^6S) + C_3H_8 ground state asymptote are based on ab initio calculations (B3LYP/HW/6-311++G(3df,-3p), see Table 4). Heavy horizontal lines indicate experimentally measured values.

An alternative pathway to form the same $(CH_4)Mo^+(C_2H_4)$ intermediate is initial primary C−H bond activation to form $H-Mo^+-1-C_3H_7$ followed either by sequential transfer of the methyl group to Mo^+ to form the $(H)(CH_3)Mo^+(C_2H_4)$ intermediate followed by reductive elimination to yield $(CH_4)Mo^+(C_2H_4)$ or by a four-centered transition state that transfers the methyl group directly to the hydrogen ligand. As noted above, primary C−H bond activation in propane is limited by ^{4}TS1(1), lying 0.64 eV above ground state reactants, which is also in reasonable agreement with the experimental threshold for methane elimination of 0.75 ± 0.12 eV. From the $H-Mo^+-1-C_3H_7$ intermediate, ^{4}TS7 was located for activation of a C−C bond to form the $(H)(CH_3)Mo^+(C_2H_4)$ intermediate on the quartet potential energy surface. The transition state is calculated to lie 0.41 eV above and the intermediate 0.39 eV below ground state reactants, Table 4 and Figure 9. The structures of these species are shown in Figure 10, and Table S4 in the Supporting Information provides more complete structural information. In the transition state, the methyl group has long bonds to both the carbon and molybdenum atoms, again a consequence of the directionality of the sp^3 hybrid orbital. In the intermediate, the Mo−H and $Mo-CH_3$ bond lengths and $H-Mo-CH_3$ bond angle are comparable to the $H-Mo^+-R$ species in Figure 2, indicating that these species are covalently bound to molybdenum. To compensate, the Mo−C bonds to ethene are much longer than in $Mo^+(C_2H_4)$ ($^4B_2$) and more similar to the sextet state (e.g., compare to the quartet and sextet states of $(CH_4)Mo^+(C_2H_4)$ in Figure 8). Several attempts to locate TS8, the transition state that connects the $(H)(CH_3)Mo^+(C_2H_4)$ and $(CH_4)Mo^+(C_2H_4)$ intermediates, were made, but these calculations always collapsed to ^{4}TS6. The estimated energy of 0.46 eV listed in Table 4 comes from a structure that nearly converged (rms force = 0.000696 hartree/bohr), shown in Figure 10, and has an imaginary frequency (1130 cm^{-1}) with the correct motion of the transferring hydrogen atom. Note that the $Mo-CH_3$ bond has lengthened while the Mo−C bonds to ethene have decreased compared to the $(H)(CH_3)Mo^+(C_2H_4)$ intermediate. Overall, Figure 9 shows that this pathway for methane

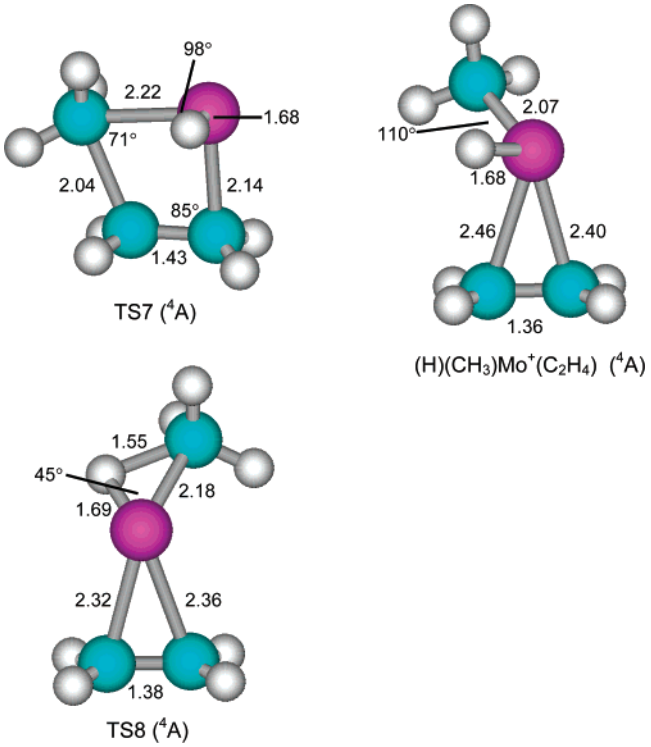

Figure 10. Structures of several intermediates and transition states relevant to CH bond activation leading to $Mo^+(C_2H_4) + CH_4$ along the sextet and quartet surfaces of the $[Mo,3C,8H]^+$ system calculated at the B3LYP/HW/6-311++G(3df,3p) level of theory. Bond lengths are given in Å.

elimination is limited by the C−H bond activation step at ^{4}TS1(1). Once past this point, CH_4 elimination is estimated to be limited by ^{4}TS8 and will compete with dehydrogenation, which is limited by ^{4}TS2.

Attempts to find a more direct four-centered transition state, TS9, that transfers a methyl group between the H−Mo^+−1-C_3H_7 and $(CH_4)Mo^+(C_2H_4)$ intermediates led to collapse to ^{4}TS7. A calculation that came close to converging gave a structure lying about 1.5 eV above the ground state reactants. This result is consistent with recent calculations[13] and the results above, which suggest that alkyl migrations are higher energy pathways than H shifts. It also verifies that this concerted pathway is higher in energy than the sequential transfer through TS7 and TS8, Figure 9.

The two pathways for elimination of methane, proceeding through initial C−C and initial C−H bond activation, cannot be distinguished on the basis of the experiments (nor would deuterium labeling experiments distinguish the mechanisms). Intuitively, the pathway through the CH_3−Mo^+−C_2H_5 intermediate seems more probable, Figure 7. If so, then the inefficiency of methane elimination (C−C bond cleavages account for only 3% of the total reactivity at thermal energies in the propane system)[1] can be explained by the relative amounts of initial C−H vs C−C bond activation. This propensity is presumably controlled by the relative energies of the insertion transition state, which is consistent with the relative energies of the rate-limiting transition states in the propane system. ^{4}TS1, which controls C−H bond activation, lies 0.43−0.64 eV above reactants, whereas ^{6}TS3, which controls C−C bond activation, lies 0.89 eV above the reactants. These values compare favorably with the experimentally measured thresholds for H_2 and CH_4 elimination of 0.41 ± 0.05 and 0.75 ± 0.12 eV, respectively.[1] Alternatively, if methane elimination occurs from the HMo^+−1-C_3H_7 intermediate, Figure 9, then the

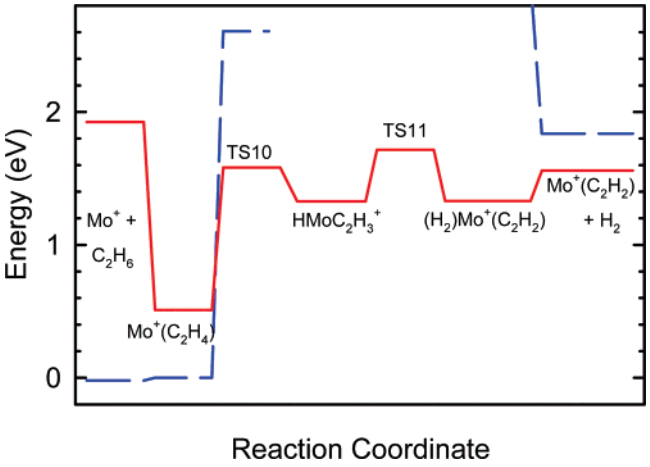

Figure 11. $[Mo,2C,4H]^+$ potential energy surfaces for CH bond activation leading to $Mo^+(C_2H_2) + H_2$ derived from theoretical results. Sextet spin surfaces are indicated by the blue dashed line and quartet spin surfaces by the red full line. The energies of all species relative to the Mo^+ (^{6}S) + C_2H_4 ground state asymptote are based on ab initio calculations (B3LYP/HW/6-311++G(3df,-3p), see Table 5).

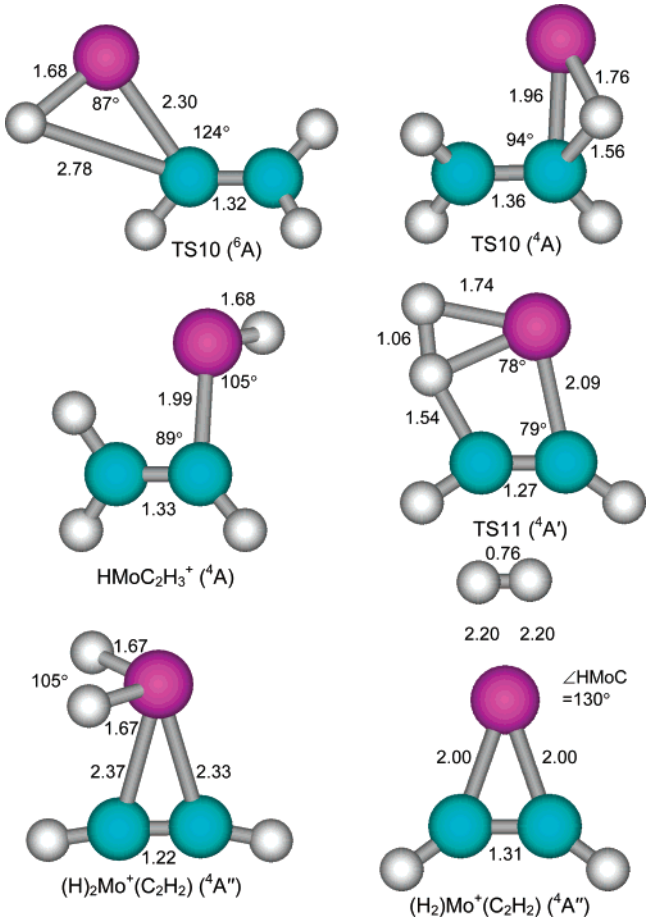

Figure 12. Structures of several intermediates and transition states relevant to CH bond activation leading to $Mo^+(C_2H_2) + H_2$ along the sextet and quartet surfaces of the $[Mo,2C,4H]^+$ system calculated at the B3LYP/HW/6-311++G(3df,3p) level of theory. Bond lengths are given in Å.

thresholds for H_2 and CH_4 elimination are limited by ^{4}TS1(2) and ^{4}TS1(1), calculated to lie at 0.46 and 0.64 eV. This is plausibly in agreement with the experimental observations, although the difference seems small compared to the experimental difference in thresholds. In this mechanistic scenario,

Table 5. Theoretical Energies of $[Mo,2C,4H]^+$ Intermediates, Transition States, and Products Calculated at the B3LYP/HW/6-311++G(3df,3p) Level of Theory

species	state	$s(s+1)$	energy (E_h)	ZPE (E_h)[a]	E_{rel} (eV)[b]
$MoC_2H_4^+$	$^6A_1$	8.76	−145.828398	0.052410	0.000
	$^4B_2$	3.78	−145.809031	0.051794	0.510
$MoH^+ + C_2H_3$	$^5\Sigma^+ + {}^2A'$	6.03 + 0.75	−145.670164	0.040820	3.994
$MoC_2H_3^+ + H$	$^5A'' + {}^2S$	6.09 + 0.75	−145.667916	0.040557	4.051
$MoC_2H^+ + H + H_2$	$^5\Sigma^+ + {}^2S$	6.04 + 0.75	−145.611002	0.027579	5.166
TS10	^4A	3.78	−145.763306	0.045383 (916)	1.582
	^6A	8.78	−145.723205	0.042967 (92)	2.608
$HMoC_2H_3^+$	^4A	3.79	−145.775542	0.045065	1.241
TS11	$^4A'$	3.78	−145.755133	0.042078 (983)	1.715
$(H_2)Mo^+(C_2H_2)$	$^4A''$	3.78	−145.770915	0.042060	1.286
$(H)_2Mo^+(C_2H_2)$	$^4A''$	3.78	−145.740018	0.039500	2.058
$Mo^+(C_2H_2) + H_2$	$^4A_2 + {}^1\Sigma_g^+$	3.78 + 0.00	−145.757568	0.038732	1.559
	$^6A_1 + {}^1\Sigma_g^+$	8.75 + 0.00	−145.745968	0.037310	1.837

[a] Zero-point energy. Imaginary frequencies are listed in parentheses in units of cm^{-1}. [b] Energy relative to the ground state species for each compound including zero-point energies (scaled by 0.989).

the relative amounts of C−H vs C−C bond activation are controlled both by the relative amounts of secondary (which leads to H_2 loss exclusively) and primary (which leads to both H_2 and CH_4 loss) C−H bond activation and by the observation that ^{4}TS2(1) leading to H_2 loss at −0.07 eV is much lower in energy than the pathway for CH_4 loss, ^{4}TS7 and ^{4}TS8, which lie at 0.41 and 0.46 eV, respectively.

C−H Bond Activation in Ethene: $MoC_2H_2^+ + H_2$ Formation. In the previous paper,[1] dehydrogenation of $MoC_2H_4^+$ to yield $MoC_2H_2^+$ was observed in both the ethane and propane systems. In the latter system, the observed threshold clearly did not correspond to the thermodynamic limit, and there were some indications that this was also true in the ethane system. The potential energy surface for dehydrogenation of $MoC_2H_4^+$ is shown in Figure 11. Structures of these species are shown in Figure 12, and Table S5 in Supporting Information provides more complete structural information. The lowest energy pathway lies along the quartet surface, with the sextet surface considerably higher. Thus, a spin change is required to move from the $^6A_1$ ground state of $Mo^+(C_2H_4)$ to the quartet surface, eventually leading to $Mo^+(C_2H_2)$ ($^4A_2$) + H_2. On the quartet surface, the reaction proceeds by C−H bond activation to form the $HMoC_2H_3^+$ intermediate, followed by coupling of two hydrogens to directly form $(H_2)Mo^+(C_2H_2)$. The structures are similar to the analogues in Figure 2 except that the CC and MoC bonds are shorter in the $[Mo,2C,4H]^+$ system, correctly reflecting the higher bond orders involved. Both the C−H bond activation step, TS10, and the four-centered transition state leading to H_2 elimination, TS11, are fairly high in energy, with the latter calculated to lie 0.13 eV higher than TS10, Table 5. TS10 on the sextet surface was also located; however, this species is particularly floppy because there is no covalent bond between the MoH^+ ($^5\Sigma^+$) and C_2H_3 ($^2A'$) components, such that verification that this is the correct transition state was difficult. Nevertheless, this species lies more than 1.0 eV above ^{4}TS10, as anticipated.

Alternatively, dihydrogen elimination from the $HMoC_2H_3^+$ intermediate could proceed by sequential hydrogen atom transfer through a $(H)_2Mo^+(C_2H_2)$ dihydride intermediate. Such an intermediate was located 2.06 eV above $Mo^+(C_2H_4)$ ($^6A_1$) and 0.34 eV above TS11, such that this pathway cannot be a lower energy pathway for dehydrogenation of ethene.

Overall, the calculated potential energy surface shows that there is a barrier of 0.16 eV in excess of the overall endothermicity. This suggests that the $Mo^+-C_2H_2$ BDE of 1.87 ± 0.05 eV measured in the previous paper is indeed a lower limit. When adjusted by this theoretical barrier, the experimental BDE becomes 2.03 ± 0.05 eV, which is more comparable to the $Mo^+-C_3H_4$ BDE of 2.22 ± 0.03 eV. As noted above, the longer chain hydrocarbon generally has lower energy intermediates and transition states such that dehydrogenation of propene to form $Mo^+(C_3H_4)$ is plausibly limited by the overall endothermicity.

High-Energy Processes: R^+, MoH^+, and MoR^+ Formation. At higher energies, formation of $C_3H_7^+$, MoH^+, $MoCH_3^+$, and $MoC_2H_5^+$ products is observed in the reactions with ethane and propane. In all cases, these species begin to dominate the product spectrum once they are energetically allowed, although in all cases they undergo further dehydrogenation reactions at still higher energies. The former two products can clearly be explained by Mo−C bond cleavage from the $H-Mo^+-C_xH_{2x+1}$ intermediates, whereas the latter two species can arise from Mo−C bond cleavage from the $CH_3-Mo^+-C_{x-1}H_{2x-1}$ intermediates. As these bond cleavages are simpler processes than the complicated rearrangements leading to dehydrogenation and alkane elimination, the former products are entropically favored and therefore dominate once energetically allowed. Furthermore, the long-range interactions between the products formed in these reactions are attractive, such that thresholds for the formation of the high-energy products should correspond to the asymptotic energies of the products. This is in agreement with the thermochemistry derived, as discussed in detail in Paper I.[1]

Conclusion

In paper I, thermodynamic arguments were used to postulate that dehydrogenation of ethane and propane by atomic molybdenum cations in their ^6S ground state was limited by barriers in excess of the overall reaction energetics. A theoretical

investigation of the reaction mechanisms for these C−H bond activation processes at the B3LYP/HW/6-311++G(3df,3p) level of theory demonstrates the veracity of this conjecture. The theoretical studies indicate that C−H bond activation processes are limited by the initial C−H bond activation step (oxidative addition to Mo^+), with a quartet spin transition state, ^{4}TS1, having an energy in reasonable agreement with experimental observations. It is found that the system must switch from the sextet surface of the ground state reactants to the quartet surface shortly before the rate-limiting transition state. ^{4}TS1 lies above both the sextet and quartet states of the Mo^+(alkene) product ions such that either are plausibly formed in the reactions.

For C−C bond activation leading to $MoCH_2^+$ formation ($+CH_4$ for ethane, $+C_2H_6$ for propane), the rate-limiting transition state, ^{6}TS3, corresponds to the initial C−C bond activation but is now located on the sextet surface. Because of the directionality of the sp^3-hybridized orbital on the methyl group, the relative energy of the transition state on the quartet surface is raised compared with the analogous TS involving the spherical hydrogen atom. This is because the molybdenum cation binds covalently to both fragments in the quartet state, whereas on the sextet surface, one of the fragments is electrostatically bound to Mo^+ such that the energy is largely unaffected upon substitution of CH_3 for H. In this mechanistic pathway, the system must switch to the quartet surface shortly after ^{6}TS3 in order to form $MoCH_2^+$ ($^4B_1$). For the other low-energy C−C bond activation process observed in the propane system, methane elimination to form $Mo^+(C_2H_4)$, the calculations show that this can plausibly occur by either initial C−C or primary C−H bond activation. The former pathway seems more consistent with the experimental measurements of the barrier heights, but the latter mechanism cannot be eliminated. For both C−H and C−C bond activation processes, the appreciable size of the experimental cross sections (Paper I)[1] demonstrates that the efficiency of the spin change is relatively high.

Acknowledgment. This research is supported by the National Science Foundation, Grant No. CHE-0451477.

Supporting Information Available: Tables S1−S5 contain theoretical structures of $[Mo,2C,6H]^+$, $[Mo,3C,8H]^+$, and $[Mo,2C,4H]^+$ intermediates and transition states calculated at the B3LYP/HW/6-311++G(3df,3p) levels of theory. This material is available free of charge via the Internet at http://pubs.acs.org.

OM700578Q